Microwave signatures of Majorana states in a topological Josephson junction

Jukka I. Väyrynen, Gianluca Rastelli, Wolfgang Belzig, and Leonid I. Glazman

Phys. Rev. B **92**, 134508 — Published 12 October 2015

DOI: 10.1103/PhysRevB.92.134508

Microwave signatures of Majorana states in a topological Josephson junction

Jukka I. Väyrynen,[1] Gianluca Rastelli,[2,3] Wolfgang Belzig,[3] and Leonid I. Glazman[1]

[1] *Department of Physics, Yale University, New Haven, CT 06520, USA*
[2] *Zukunftskolleg, Universität Konstanz, D-78457 Konstanz, Germany*
[3] *Fachbereich Physik, Universität Konstanz, D-78457 Konstanz, Germany*

(Dated: June 29, 2015)

We find the admittance of a topological Josephson junction $Y(\omega, \varphi_0, T)$ as a function of frequency ω, the static phase bias φ_0 applied to the superconducting leads, and temperature T. The dissipative part of Y allows for spectroscopy of the sub-gap states in the junction. The resonant frequencies $\omega_{\mathcal{M},n}(\varphi_0)$ for transitions involving the Majorana ($\mathcal{M}$) doublet exhibit characteristic kinks in the φ_0-dependence at $\varphi_0 = \pi$. The kinks – associated with decoupled Majorana states – remain sharp and the corresponding spectroscopic lines are bright at any temperature, as long as the leads are superconducting. The developed theory may help extracting quantitative information about Majorana states from microwave spectroscopy.

The interest in the condensed matter realizations of Majorana states is fueled by the promise of topologically-protected quantum computing [1–4]. While the latter requires the ability to braid the states, the current experimental effort [5–12] focuses on indications of the Majorana states' presence in various implementations of topologically-nontrivial superconductors. The majority of experiments use the dc electron transport spectroscopy and aim at detecting a zero-bias conductance peak associated with tunneling into a Majorana state [13–15] or the 4π-periodic phase dependence of the two "Majorana branches" formed by an occupied and unoccupied Majorana doublet [6, 16, 17]. In the former case, some additional checks are necessary [5] to exclude other sources (*e.g.*, Kondo effect) of the zero-bias anomaly [8, 18, 19]. Attempts to observe the unusual phase dependence rely on the absence of inter-branch relaxation; this is hard to enforce, especially over an extended time period required in the interference experiments [10–12, 20], or at higher bias voltage needed for observation of multiple Shapiro steps [6].

Limitations of the techniques implemented to-date give an incentive to search for alternatives. Our theory elucidates the manifestations of the Majorana states in the microwave spectrum of a topological Josephson junction. Spectroscopy of the Andreev (*i.e.*, sub-gap) states was performed recently in experiments with conventional metallic break junctions [21, 22]. The experiments did detect the transitions from an Andreev level to the continuum of quasiparticle states [22], and the transitions between the two discrete Andreev levels [21]. The latter result in a narrow bright line in the spectrum, especially attractive for spectroscopy. This is why we also aim at a setup allowing for discrete lines in the spectrum of a topological Josephson junction. The junction hybridizes the two Majorana states to form two levels differing by the parity of electron number. Therefore, the particle number-preserving interaction with microwaves does not cause transitions within this doublet. That prompts us to consider junctions of length $L \gtrsim \xi$ allowing for higher-energy Andreev states, along with the Majorana doublet (here ξ is the coherence length in the topological superconductor).

We focus on the contribution of the discrete, sub-gap states to the admittance $Y(\omega, \varphi_0, T)$ of a topological Josephson junction [23]. The setup for the junction is sketched in Fig. 1 and is based on a two-dimensional topological insulator [17] or a semiconductor nanowire [24, 25] with strong spin-orbit (SO) interaction in proximity with a conventional superconductor. The junction is controlled by the static order parameter phase difference φ_0 between the leads and is probed by applying a small voltage $V(t)$ induced by microwaves [26]. It creates a weak time-dependent perturbation $\delta\varphi(t)$ of the phase difference, $d(\delta\varphi)/dt = (2e/\hbar)V(t)$, which drives the transitions between the sub-gap levels. The lowest doublet is formed by the hybridized Majorana states. Their crossing at $\varphi_0 = \pi$ is protected by conservation of electron number parity. (At the crossing, the number parity of the ground state switches between even and odd, see Fig. 2a.) The crossings of the higher-energy Andreev levels are not protected by the parity. In a generic junction, these crossings are avoided, resulting in a smooth dependence of the corresponding energies $E_n(\varphi_0)$ on φ_0, see Fig. 2a.

We find the discrete lines in the microwave absorption spectrum originating from the transitions in the sub-gap energy domain. The transitions involving the states of the Majorana doublet, see Fig. 2a, result in a series of lines with a characteristic kink at $\varphi_0 = \pi$ in the dependence of the transition frequencies on φ_0,

$$\hbar\omega_{\mp\mathcal{M},n}(\varphi_0) = E_n(\pi) \mp E'_{\mathcal{M}}|\varphi_0 - \pi| + \mathcal{O}[(\varphi_0 - \pi)^2]\,. \quad (1)$$

Here $\mp E'_{\mathcal{M}} = \mp dE_{\mathcal{M}}/d\varphi_0$ are the slopes at $\varphi_0 = \pi$ of the energies of the two Andreev levels formed by the occupied and unoccupied Majorana doublet at the level crossing point, $E_n(\pi)$ is the energy of the higher Andreev level, and the last term in Eq. (1) represents the smooth part of its φ_0-dependence. The intensity of these lines is quantified by $\mathrm{Re}Y(\omega, \varphi_0, T)$, for which in the vicinity of $\varphi_0 = \pi$

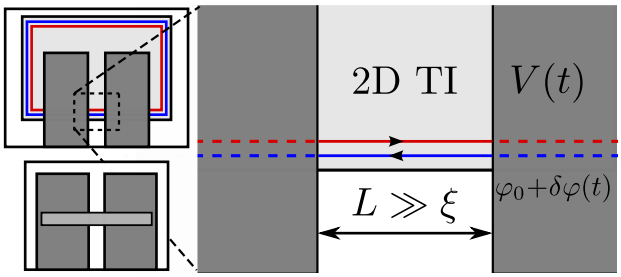

FIG. 1. (Color online) **Right:** A typical junction setup hosting Majorana states. The arrowed lines mark the gapless helical edge modes of the 2D topological insulator (2D TI, light grey area), proximity coupled (dashed lines) to the left and right superconducting leads (grey area). The junction and the leads are wider than the coherence length ξ of superconductivity induced in the TI; ξ sets the scale for the bound states' decay length into the leads. A weak time-dependent voltage $V(t)$ applied between the leads gives rise to a small component, $\delta\varphi(t) \ll 1$, modulating the superconducting phase difference across the junction (in the figure, the left lead is grounded). The resulting current response contains signatures of Majorana bound states. **Upper left inset:** The full setup; the outer junction can be ignored since it is much longer then the inner one and gives a signal weaker by a factor $(L/L_{\rm outer})^2$, see Eq. (12). **Lower inset:** The Majorana detection scheme is also applicable to a junction formed by a topological semiconductor nanowire (light grey).

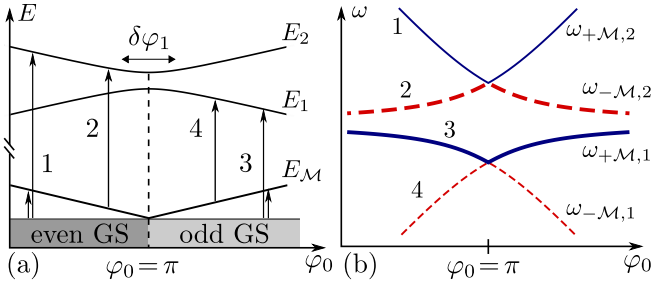

FIG. 2. (Color online) The low-lying excitations spectrum (a) and the absorption spectrum (b) of a topological Josephson junction. (a) The dependence of the first three Andreev levels in the junction on the phase φ_0. The lowest level has zero energy $E_{\mathcal{M}}$ at $\varphi_0 = \pi$, corresponding to two decoupled Majorana bound states. At $\varphi_0 = \pi$ the electron number parity of the ground state (GS) changes. Energy $E_{\mathcal{M}}$ has a discontinuous φ_0-derivative (a kink) at the GS switching point. The lines $E_{1,2}(\varphi_0)$ for higher levels are smooth, as the degeneracies are lifted by backscattering ($\delta\varphi_1$ characterizes the avoided crossing). The kink in the $E_{\mathcal{M}}(\varphi_0)$ function can be probed by microwave spectroscopy. The transitions conserving the electron number parity are shown by arrows 1 through 4 and give rise to spectroscopic lines. (Transitions 1 and 3 create a *pair* of quasiparticles above the GS.) (b) The absorption lines near $\varphi_0 = \pi$, see Eq. (1). At $T = 0$, transitions [arrows 1 and 3 in panel (a)] start from the GS resulting in lines 1 and 3 (solid blue) each displaying a kink at $\varphi_0 = \pi$. Populated level $E_{\mathcal{M}}$ enables transitions 2 and 4 (dashed red), which also show a kink, c.f. Eq. (2). At finite temperature this results in a crossing of spectral lines at $\varphi_0 = \pi$. For the φ_0 dependence of the transitions' oscillator strengths, see Eq. (12).

we find the following estimate:

$$\mathrm{Re}\, Y(\omega,\varphi_0,T) \approx \frac{2\pi e^2}{\hbar}\frac{(E'_{\mathcal{M}})^2}{\hbar\omega}\sum_{E_n>E_{\mathcal{M}}}\sum_{\sigma=\pm} \times\left[\tanh\frac{E_n(\pi)}{2T}-\tanh\frac{E_n(\pi)-\hbar\omega}{2T}\right]\delta(\hbar\omega_{\sigma\mathcal{M},n}(\varphi_0)-\hbar\omega). \quad (2)$$

Note that unlike the zero-bias anomalies in dc transport, the spectroscopic feature associated with the kink in the φ_0-dependence of $\omega_{\mp\mathcal{M},n}(\varphi_0)$ is not broadened by temperature. The brightness of lines depends weakly on temperature, with the scale provided by the higher-energy levels E_n. The admittance we find is a linear-response property of the junction; unlike the Shapiro-steps manifestation of the Majoranas, their effect on Y does not set any stringent requirement on the relaxation time of the system to its equilibrium state. Our main results, Eqs. (1) and (2), are illustrated in Fig. 2b. In the following, we outline their derivation and application to concrete junction models.

A microwave field induces voltage bias $V(t)$ between the leads of a device built on a basis of a two-dimensional topological insulator (TI) or a nanowire (NW), see Fig. 1. The bias excites current $\langle\hat{I}(t)\rangle$ between the leads, connected by the NW or the edge states of a TI. The admittance $Y(\omega)$ of the device is defined as a response function, $\langle\hat{I}(\omega)\rangle = Y(\omega)V(\omega)$, at frequency ω. For the current operator, we may take the current through the junction between the TI (or NW) and the right lead, $\hat{I}(t) = e\cdot d\hat{N}_R/dt$. Here $\hat{N}_R$ is the number of electrons of the edge state in TI (or of NW) which tunneled into the right superconducting lead.

We are interested in transitions between the states with energies below the proximity-induced gap Δ_0; the latter inevitably is smaller than the superconducting gap in the leads which are the sources of proximity. That allows us to use the effective Hamiltonian of a proximized TI (or NW) instead of the full Hamiltonian in the evaluation of $d\hat{N}_R/dt$ [27]. The effective Hamiltonian $\hat{H}^{(0)} = \int dx\Psi^\dagger\mathcal{H}^{(0)}\Psi/2$ in Nambu representation (parametrized by matrices τ) takes the form

$$\mathcal{H}^{(0)}(x) = -i\hbar v\tau_z\sigma_z\partial_x - \mu\tau_z + V(x)\tau_z + M(x)\sigma_x + \Delta_0(x)[\tau_x\cos\varphi(x) - \tau_y\sin\varphi(x)]\,. \quad (3)$$

The first term here is the electron kinetic energy, μ is the chemical potential, $V(x)$ is the scalar potential (induced, *e.g.*, by disorder), and $M(x)$ is the Zeeman splitting in the junction; the 4×4 matrix Hamiltonian $\mathcal{H}^{(0)}$ describes here a helical edge state in a TI [17]. (We show below that the effective Hamiltonian of a NW in a sufficiently large magnetic field takes the same form, see the paragraph preceding Eq. (13).) We assume the leads to be wide compared to the proximity-induced coherence length $\xi =$

$\hbar v/\Delta_0$ [28]. That allows us to replace the leads depicted in Fig. 1 by semi-infinite pads,

$$\Delta_0(x) = \Delta_0[\Theta(-x) + \Theta(x-L)]\,,\ \varphi(x) = \varphi_0\Theta(x-L)\,, \tag{4}$$

where L is the length of the junction. We set the order parameter of the left lead to be real so that φ_0 is the phase difference across the junction. Using Eq. (3) to evaluate dN_R/dt, we find

$$\hat{I} = (2e/\hbar)(\partial\hat{H}^{(0)}/\partial\varphi_0)\,. \tag{5}$$

for the current operator projected on the manifold of states with energy below the gap in the superconducting leads. It will be used below to derive the contribution to admittance coming from the transitions between the discrete sub-gap states.

Application of a bias $V(t)$ to the junction results in a time-dependent addition $\delta\varphi(t)$ to the static phase bias φ_0. According to the Josephson relation, $\delta\dot{\varphi}(t) = 2eV(t)/\hbar$. For a monochromatic bias voltage $V(t) = V(\omega)\cos\omega t$, we can treat $\delta\varphi(t)$ perturbatively as long as $|eV(\omega)/\hbar\omega| \ll 1$. (Hereinafter, we set $\hbar = 1$.) In this weak bias limit, the Hamiltonian H can be split into a time-independent part $H^{(0)}$, and a time-dependent perturbation

$$H^{(1)}(t) = \delta\varphi(t)(\partial H^{(0)}/\partial\varphi_0)\,. \tag{6}$$

To evaluate the admittance $Y(\omega)$, we apply the standard linear response theory to the problem set by Eqs. (3)-(6). The result may be expressed in terms of the spectrum E_n of $\mathcal{H}^{(0)}$ and the matrix elements

$$\mathcal{H}^{(1)}_{m;n} = \int dx \Phi^*_m(x)[\partial_{\varphi_0}\mathcal{H}^{(0)}(x)]\Phi_n(x) \tag{7}$$

of the operator defining the perturbation, see Eq. (6). Here $\Phi_n(x)$ are the eigenfunctions of $\mathcal{H}^{(0)}$, and energies E_n are measured from the Fermi level. We are interested in the transitions between the sub-gap states, so the corresponding wave functions decay exponentially at $|x| \to \infty$. As the result of using the Nambu spinor notation, the energy spectrum is particle-hole symmetric (PHS), meaning that the eigenvalues come in pairs $(E_n, -E_n)$. We will label by $-n$ the state with energy $-E_n$ for all $n \geq 0$; the lowest ($n = 0$) doublet is $(E_{\mathcal{M}}, -E_{\mathcal{M}})$. We concentrate on the absorption lines which originate from transitions involving a state of this doublet. Using the Kubo formula [29] and PHS, we obtain for the corresponding part of the admittance:

$$\mathrm{Re}\, Y(\omega) = \frac{4\pi e^2}{\omega}\sum_{E_n > E_{\mathcal{M}}}\left[\tanh\frac{E_n}{2T} - \tanh\frac{\omega - E_n}{2T}\right] \times\left\{|\mathcal{H}^{(1)}_{\mathcal{M};n}|^2\delta(\omega - \omega_{-\mathcal{M},n}) + |\mathcal{H}^{(1)}_{-\mathcal{M};n}|^2\delta(\hbar\omega - \omega_{+\mathcal{M},n})\right\}. \tag{8}$$

Here $\omega_{\mp\mathcal{M},n} = E_n \mp E_{\mathcal{M}}$, see Eq. (1). Note that there are no terms with $E_n = E_{\mathcal{M}}$ since $\mathcal{H}^{(1)}_{\mathcal{M};-\mathcal{M}} = 0$ by Pauli exclusion principle. The eigenvalues E_n with $n \neq 0$ are in general not degenerate, contrary to the case of a conventional time-reversal symmetric (TRS) S-N-S junction, where the states are doubly degenerate (Kramers doublets). The "degeneracy" and zero value of the energy $E_{\mathcal{M}}$ at $\varphi_0 = \pi$ are protected by symmetries, and will be discussed below. Equation (8) was derived in linear response theory. It assumes that the perturbation (6) is weak enough to allow the system to relax to equilibrium between the acts of the microwave photon absorption. Relaxation may happen through recombination of the excited quasiparticles by emission of phonons or photons into the environment [30]. A finite recombination rate would result in Lorentzian broadening of the spectral lines in Fig. 2b.

The junction sub-gap excitation spectrum is found from Eqs. (3) and (4) by using the standard scattering matrix method [31]. We find that there is always a state with vanishing energy $E_{\mathcal{M}}$ at $\varphi_0 = \pi$ [26]. The $E_{\mathcal{M}} = 0$ state is protected by fermion number parity conservation. (We assume the junction is well separated from other junctions or interfaces with bound states, allowing us to ignore hybridization of those states with $E_{\mathcal{M}}$, see Fig. 1 and footnote [27].) Near $\varphi_0 = \pi$ the dispersion $E_{\mathcal{M}}(\varphi_0)$ is linear. For a reflectionless junction [$M = 0$ in Eq. (3)] we find

$$E_{\mathcal{M}}(\varphi_0) = \frac{1}{2}\frac{v}{L+\xi}|\varphi_0 - \pi|\,. \tag{9}$$

Breaking of TRS in the junction, $M \neq 0$, results in backscattering. This does not lead to qualitative changes to Eq. (9) but merely modifies the prefactor in it [32].

The situation is different for the higher Andreev levels. In a reflectionless junction they have degeneracies [33] at $\varphi_0 = \pi$: in our notation, for *odd* n the levels n and $n+1$ are degenerate, $E^{(0)}_n(\pi) = E^{(0)}_{n+1}(\pi) = (n+1)\pi v/2L$. (We take now $L \gg \xi$.) Backscattering lifts these degeneracies and thus leads to qualitative changes in the spectrum at $\varphi_0 = \pi$ (see Fig. 2a). The resulting avoided crossing makes the φ_0-dependence of the levels' energies smooth [34]

$$E_n(\varphi_0) = E^{(0)}_n(\pi) + (-1)^n\frac{v}{2L}\sqrt{(\varphi_0 - \pi)^2 + (\delta\varphi_n)^2}\,. \tag{10}$$

(We ignore here corrections to the prefactor $v/2L$ due to weak backscattering.) The smoothness in (10) is characterized by the width of the avoided-crossing region $\delta\varphi_n = \left|r_+ + r^*_-\right|_{E=E^{(0)}_n(\pi)}$. We denote by $r^{(\prime)}_{+/-}(E)$ the reflection amplitudes for electrons/holes entering the junction from the left (right) at energy E. In a simple model with $V(x) = 0$, $M(x) = M\Theta(x)\Theta(L-x)$, and $M \ll v/L$, the junction is symmetric and $r_\pm(E) = M(1 - e^{2i(E\pm\mu)L/v})/2(E \pm \mu)$. In this model, for small

chemical potential, $\mu \ll v/L$, the width of the avoided crossing is [35]

$$\delta\varphi_n = \frac{|M|}{v/2L}\frac{|\mu|}{E_n^{(0)}(\pi)}\,. \tag{11}$$

The sub-gap spectrum determines the resonance frequencies $\omega_{\mp\mathcal{M},n}(\varphi_0)$: combining Eqs. (9) and (10) yields Eq. (1). The brightness of the spectral lines is set by the matrix elements in Eq. (8). They are calculated from Eq. (7) where, according to Eq. (4), the integration over x is restricted to the right superconducting region $x > L$ where $\partial_{\varphi_0}\mathcal{H}^{(0)}(x)$ is non-zero. There, the sub-gap wave functions decay exponentially, $\Phi_n(x) = e^{-(x-L)/\xi}\Phi_n(L)$. We assume here $E_n \ll \Delta_0$ so that the decay length is approximated by ξ. In the limit of weak reflection, we find [26]

$$|\mathcal{H}^{(1)}_{\pm\mathcal{M};n}|^2 = \frac{v^2}{8L^2}\left[1 \pm (-1)^n \frac{|\varphi_0-\pi| \pm 2\mathrm{Re}\delta\Phi^*_{\mathcal{M}}\delta\varphi_n e^{i\vartheta_n}}{\sqrt{(\delta\varphi_n)^2+(\varphi_0-\pi)^2}}\right]. \tag{12}$$

Importantly, $|\mathcal{H}^{(1)}_{\pm\mathcal{M};n}|^2 \propto 1/L^2$; likewise, the contribution in the admittance from the long outer junction in Fig. 1 is proportional to $1/L^2_{\rm outer}$ and can be ignored since the corresponding length $L_{\rm outer} \gg L$. In Eq. (12) $\vartheta_n = \arg(r'_+ + r'^*_-)_{E=E_n^{(0)}(\pi)}$ and $\delta\Phi_{\mathcal{M}} = \frac{v}{2L}[d_+^2\partial_E r^*_+]_{E=0}$ is the small correction (due to backscattering) to the wave function of level $E_{\mathcal{M}}$; here $d_\pm$ is the transmission amplitude. In the simple model used to derive Eq. (11), $\delta\Phi_{\mathcal{M}} = \frac{M}{v/L}(\frac{1}{2} + \frac{i}{3}\frac{\mu}{v/L})$.

Since Eq. (12) was derived assuming $L \gg \xi$, we can express its prefactor as $(E'_{\mathcal{M}})^2/2$ by using Eq. (9) in that limit; the replacement is valid if the levels resolved in the transitions are far below Δ_0. Furthermore, close to $\varphi_0 = \pi$ we can neglect the second term in the square brackets in (12) as long as $|\varphi_0 - \pi| \ll \delta\varphi_n$, since $|\delta\Phi_{\mathcal{M}}| \ll 1$. Using the approximate matrix elements in Eq. (8) leads to Eq. (2).

Approximating the matrix elements in Eq. (2) by a constant $(E'_{\mathcal{M}})^2/2$ does not capture the brightness variations of the absorption lines with n and φ_0. At $\varphi_0 = \pi$ transitions to levels E_n with *odd* n (lines 3 and 4 in Fig. 2b) are brighter than transitions to levels E_{n+1} (lines 1 and 2), due to $\delta\Phi_{\mathcal{M}} \neq 0$. As a function of φ_0, the brightness is non-analytic at $\varphi_0 = \pi$ which is a maximum (minimum) for lines 1 and 4 (2 and 3) in Fig. 2b. Far from the avoided crossing, $|\varphi_0 - \pi| \gg \delta\varphi_n$, the spectral lines 1 and 4 become dim. In general, the lines corresponding to frequencies $\omega_{-\mathcal{M},n}$ and $\omega_{+\mathcal{M},n+1}$ with n *odd* become dim away from $\varphi_0 = \pi$. This is because of an approximate selection rule for the matrix elements $\mathcal{H}^{(1)}_{\pm\mathcal{M};n}$: we see from Eq. (12) that $|\mathcal{H}^{(1)}_{\mathcal{M};n}|^2$ and $|\mathcal{H}^{(1)}_{-\mathcal{M};n+1}|^2$ for odd n are smaller by factor $\propto \mathrm{Re}\delta\Phi^*_{\mathcal{M}}\delta\varphi_n e^{i\vartheta_n}/|\varphi_0-\pi|$ compared to those with even n. [36] This analysis allows us to extrapolate our theory to stronger backscattering, $\delta\varphi_n \sim 1$. Due to the large width of the avoided crossing, the above approximate selection rule becomes inapplicable. On the other hand, at $\varphi_0 = \pi$ the alternation of the lines' intensities with n becomes more pronounced. The main feature, the kink in the transition frequencies $\omega_{\mp\mathcal{M},n}(\varphi_0)$ at $\varphi_0 = \pi$, persists.

We derived Eqs. (1) and (2) for a TI junction, but the same low-energy model, Eqs. (3)-(10), is applicable to a NW-based setup. For illustration, we concentrate here on the limit of large Zeeman energy, $B \gg m\alpha^2$; the SO energy scale here is determined by the electron effective mass m and SO velocity α. At low-energies $E \ll B$, linearization [37] of the spectrum near the Fermi points $k \approx \pm k_Z = \pm\sqrt{2mB}$ leads to an effective Hamiltonian of the form (3) with $v = k_Z/m$, and $\Delta_0 = \Delta 2m\alpha/k_Z$ where Δ is the induced s-wave gap in the nanowire. (We set $\mu = 0$ for simplicity.) The structure of spectrum of a long NW junction is therefore identical to that of the TI junction described above – only the microscopic forms of the phenomenological parameters in (3) are different.

In the NW junction even TRS scalar disorder may lift the degeneracies of high Andreev levels. We illustrate this by considering a short-range impurity $u_0\delta(x-L)$ in the microscopic Hamiltonian. (For definiteness, we take the impurity to be at the junction interface, as was done in Ref. 24.) The low-energy projection of the impurity Hamiltonian yields respective forward and backscattering terms [26] $V(x) \approx u_0\delta(x-L)$ and $M(x) \approx u_0\delta(x-L)$ in Eq. (3). (The prefactors here are given to lowest order in $m\alpha^2/B$.) The width of the avoided crossing,

$$\delta\varphi_n = 2\frac{|u_0|}{v}\frac{\xi}{L}\frac{E_n^{(0)}(\pi)}{v/L}\,, \tag{13}$$

is finite due to $M \neq 0$; here, as before, for n odd $E_n^{(0)}(\pi) = E_{n+1}^{(0)}(\pi) = (n+1)\pi v/2(L+\xi)$. The correction to the lowest-level wave function is $\delta\Phi_{\mathcal{M}} = (u_0/v)(1 - iu_0/v)$ and the phase appearing in Eq. (12) is $e^{i\vartheta_n} = (u_0/|u_0|)(1 - iu_0/v)$. We see that the avoided crossings and the transition matrix elements in a NW junction can be quantified in the same way as in a TI junction.

Using Eq. (9), we may compare the strength of absorption, Eq. (2), with the corresponding strength [38] of transition within the pair of Andreev levels in a conventional short S-N-S junction [21, 22]. At equal frequencies ω, the transition in the "Majorana" junction is stronger than the one in a conventional junction if the transmission coefficient of the latter is < 0.4.

In summary, we have shown how Majorana bound states manifest in the finite-frequency admittance of a topological Josephson junction with multiple Andreev levels. Our main finding is a kink in the φ_0-dependence of the resonant absorption frequency, and can be observed in the dissipative (real) part of the admittance $Y(\omega)$, see Eq. (1) and Fig. 2b. Alternatively, one may employ the reflected microwaves' phase shift, $\arg Y(\omega)$,

obtained from Eq. (8) and its Kramers-Kronig partner. The frequency-dependent phase shift jumps by π across a resonance, and the position of this jump as a function of φ_0 shows a kink. The kink is a consequence of the ground state parity switching in the junction, or decoupling of Majorana states. The admittance provides a novel, linear-response signature of this decoupling.

We thank Michel Devoret and Liang Fu for discussions, and Richard Brierley and Hendrik Meier for valuable comments on the manuscript. This work was supported by NSF DMR Grant 1206612, ONR Grant Q00704, ARO Grant W911NF-09-1-0514, DFG through SFB 767, EU FP7 Marie Curie Zukunftskolleg Incoming Fellowship Programme (Grant 291784) and the Senior Fellowship of the Zukunftskolleg, Konstanz.

[1] A. Kitaev, Annals of Physics **303**, 2 (2003).
[2] C. Nayak, S. H. Simon, A. Stern, M. Freedman, and S. Das Sarma, Reviews of Modern Physics **80**, 1083 (2008), arXiv:0707.1889 [cond-mat.str-el].
[3] J. Alicea, Reports on Progress in Physics **75**, 076501 (2012), arXiv:1202.1293 [cond-mat.supr-con].
[4] C. Beenakker, Annual Review of Condensed Matter Physics **4**, 113 (2013), http://dx.doi.org/10.1146/annurev-conmatphys-030212-184337.
[5] V. Mourik, K. Zuo, S. M. Frolov, S. R. Plissard, E. P. A. M. Bakkers, and L. P. Kouwenhoven, Science **336**, 1003 (2012).
[6] L. P. Rokhinson, X. Liu, and J. K. Furdyna, Nature Physics **8**, 795 (2012).
[7] M. T. Deng, C. L. Yu, G. Y. Huang, M. Larsson, P. Caroff, and H. Q. Xu, Nano Letters **12**, 6414 (2012), pMID: 23181691, http://dx.doi.org/10.1021/nl303758w.
[8] A. Das, Y. Ronen, Y. Most, Y. Oreg, M. Heiblum, and H. Shtrikman, Nature Physics **8**, 887 (2012), arXiv:1205.7073 [cond-mat.mes-hall].
[9] G. Koren, T. Kirzhner, E. Lahoud, K. B. Chashka, and A. Kanigel, Phys. Rev. B **84**, 224521 (2011), arXiv:1111.3445 [cond-mat.supr-con].
[10] C. Kurter, A. D. K. Finck, Y. S. Hor, and D. J. Van Harlingen, ArXiv e-prints (2013), arXiv:1307.7764 [cond-mat.mes-hall].
[11] S. Hart, H. Ren, T. Wagner, P. Leubner, M. Mühlbauer, C. Brüne, H. Buhmann, L. W. Molenkamp, and A. Yacoby, Nature Physics **10**, 638 (2014), arXiv:1312.2559 [cond-mat.mes-hall].
[12] V. S. Pribiag, A. J. A. Beukman, F. Qu, M. C. Cassidy, C. Charpentier, W. Wegscheider, and L. P. Kouwenhoven, ArXiv e-prints (2014), arXiv:1408.1701 [cond-mat.mes-hall].
[13] K. T. Law, P. A. Lee, and T. K. Ng, Phys. Rev. Lett. **103**, 237001 (2009).
[14] K. Flensberg, Phys. Rev. B **82**, 180516 (2010).
[15] J. D. Sau, S. Tewari, R. M. Lutchyn, T. D. Stanescu, and S. Das Sarma, Phys. Rev. B **82**, 214509 (2010), arXiv:1006.2829 [cond-mat.supr-con].
[16] H.-J. Kwon, V. M. Yakovenko, and K. Sengupta, Low Temperature Physics **30**, 613 (2004).
[17] L. Fu and C. L. Kane, Phys. Rev. B **79**, 161408 (2009).
[18] H. O. H. Churchill, V. Fatemi, K. Grove-Rasmussen, M. T. Deng, P. Caroff, H. Q. Xu, and C. M. Marcus, Phys. Rev. B **87**, 241401 (2013).
[19] A. D. K. Finck, D. J. Van Harlingen, P. K. Mohseni, K. Jung, and X. Li, Physical Review Letters **110**, 126406 (2013), arXiv:1212.1101 [cond-mat.mes-hall].
[20] D. M. Badiane, L. I. Glazman, M. Houzet, and J. S. Meyer, Comptes Rendus Physique **14**, 840 (2013).
[21] L. Bretheau, Ç. Girit, H. Pothier, D. Esteve, and C. Urbina, Nature **499**, 312 (2013).
[22] L. Bretheau, Ç. O. Girit, C. Urbina, D. Esteve, and H. Pothier, Phys. Rev. X **3**, 041034 (2013).
[23] As similar proposal was given in Ref. [39] where the authors consider the above-gap transitions in a nanowire with Majoranas. There the control parameter is the chemical potential of the wire.
[24] R. M. Lutchyn, J. D. Sau, and S. Das Sarma, Phys. Rev. Lett. **105**, 077001 (2010).
[25] Y. Oreg, G. Refael, and F. von Oppen, Phys. Rev. Lett. **105**, 177002 (2010).
[26] We consider a system where the phase φ_0 is classical. Our method does not require its quantum fluctuations, unlike, for example, the proposal in Ref. [40].
[27] See Supplemental Material for details. The supplement includes references to 41–44.
[28] In the case of a NW junction, we assume that the ends of the wire are much farther than ξ away from the junction. In the TI setup there are two junctions, see Fig. 1. The outer one can be ignored if it is much longer than the inner one, see remark below Eq. (12).
[29] L. Landau and E. Lifshitz, *Statistical Physics*, 3rd ed., Vol. 5 (Butterworth-Heinemann, 1980).
[30] C. Padurariu and Y. V. Nazarov, EPL (Europhysics Letters) **100**, 57006 (2012); D. G. Olivares, A. L. Yeyati, L. Bretheau, Ç. O. Girit, H. Pothier, and C. Urbina, Phys. Rev. B **89**, 104504 (2014); A. Zazunov, A. Brunetti, A. L. Yeyati, and R. Egger, Phys. Rev. B **90**, 104508 (2014).
[31] C. W. J. Beenakker, Phys. Rev. Lett. **67**, 3836 (1991).
[32] The slope is $dE_{\mathcal{M}}/d\varphi_0 = \pm\frac{1}{2}\frac{v}{L+\xi}(1+\mathcal{O}(|r_+|^2))$, see Ref. 26.
[33] We consider here free electrons; interactions can lift the degeneracy even in a TRS junction [45].
[34] Equations (9) and (10) are valid in the full range of φ_0 except for a narrow interval around $\varphi_0 = 0$ where a similar avoided crossing happens.
[35] Lifting of degeneracies in the model for which Eq. (11) was derived requires, in addition to $M \neq 0$, a non-zero chemical potential μ, due to special symmetries [26] of (3) at the Dirac point.
[36] This selection rule is exact in a reflectionless junction, $\delta\varphi_n = 0$, where the operator S_z commutes with $H^{(0)}$ and $H^{(1)}$.
[37] J. Klinovaja and D. Loss, Phys. Rev. B **86**, 085408 (2012).
[38] F. Kos, S. E. Nigg, and L. I. Glazman, Phys. Rev. B **87**, 174521 (2013).
[39] O. Dmytruk, M. Trif, and P. Simon, ArXiv e-prints (2015), arXiv:1502.03082 [cond-mat.mes-hall].
[40] E. Ginossar and E. Grosfeld, Nature Communications **5**, 4772 (2014), arXiv:1307.1159 [cond-mat.mes-hall].

[41] C. Wang, Y. Y. Gao, I. M. Pop, U. Vool, C. Axline, T. Brecht, R. W. Heeres, L. Frunzio, M. H. Devoret, G. Catelani, L. I. Glazman, and R. J. Schoelkopf, Nature Communications **5**, 5836 (2014).

[42] A. C. Potter and P. A. Lee, Phys. Rev. B **83**, 184520 (2011).

[43] C. W. J. Beenakker, D. I. Pikulin, T. Hyart, H. Schomerus, and J. P. Dahlhaus, Phys. Rev. Lett. **110**, 017003 (2013).

[44] S.-f. Zhang, W. Zhu, and Q.-f. Sun, Journal of Physics: Condensed Matter **25**, 295301 (2013).

[45] F. Zhang and C. L. Kane, Phys. Rev. Lett. **113**, 036401 (2014).